

Probing exotic long-lived particles from the prompt side using the CONTUR method

L. Corpe¹ A. Goudelis¹ S. Jeannot¹ S. Jeon²

¹*Université Clermont Auvergne, CNRS/IN2P3, LPCA, 63000 Clermont-Ferrand, France*

²*Boston University, 590 Commonwealth Avenue, Boston, Massachusetts 02215, USA*

E-mail: lcorpe@cern.ch

ABSTRACT: A method to derive constraints on new physics models featuring exotic long-lived particles using detector-corrected measurements of prompt states is presented. The CONTUR workflow is modified to account for the fraction of long-lived particles which decay early enough to be reconstructed as prompt, making it possible to determine how many of signal events would be selected in the RIVET routines which encapsulate the fiducial regions of dozens of measurements of Standard Model processes by the ATLAS and CMS collaborations. New constraints are set on several popular exotic long-lived particle models in the early-decay regime, which is often poorly covered by direct searches. The probed models include feebly-interacting dark matter, hidden sector models mediated by a heavy neutral scalar, dark photon models and a model featuring photo-phobic axion-like particles.

Contents

1	Introduction	1
2	Re-interpretation of measurements with Contur	3
3	Adapting Contur to LLP topologies	4
4	Constraints on feebly interacting DM	7
5	Constraints on hidden sector models with heavy mediators decaying into long-lived scalars	10
6	Constraints on heavy, long-lived dark photon models	13
7	Constraints on long-lived photophobic axion-like particles	14
8	Conclusions	18

1 Introduction

The discovery of the Higgs boson in 2012 closed an important chapter of the history of particle physics. But despite all the triumph of the discovery, the Standard Model (SM) is not the end of the story of fundamental physics. Indeed, the lack of a convincing candidate for Dark Matter (DM), the issue of the hierarchy problem, the matter-antimatter asymmetry of the universe, and the established fact of neutrino oscillations, all point towards the existence of new, undiscovered particles. Nevertheless, now that the first decade of LHC data has been scrutinized, no long-standing signs of new particles or interactions have come to light. This prompts the question: “are there assumptions in the LHC research programme that could be hampering a discovery?” Indeed, one possible blind spot is the existence of semi-stable new particles, which could travel far enough into the detector to leave neither missing transverse momentum signatures, nor be reconstructed as standard objects. Since the standard ATLAS and CMS reconstruction algorithms assume that activity started at the interaction point, many of these new signals could have been thrown away as noise. Besides the experimental motivation, these exotic Long-Lived Particles (LLPs) also have good theoretical credentials. Long lifetimes occur when a particle’s width becomes small, typically because of a small matrix element (for example, small couplings or heavy virtual particles mediating the decay) or phase space (for example, due to small mass differences between parent and daughter particles). These mechanisms occur frequently in the SM, and it should be expected that they would occur in a wide variety of new physics models

that resolve the fundamental questions facing particle physics, from supersymmetry [1–6] to hidden sector (HS) [7–9] and axion-like particle models [10].

Over the last decade, there has been an upsurge in interest in exotic LLP searches at the LHC [11], encompassing an impressive variety of signatures from displaced vertices and jets to anomalous ionization (see Refs [12–17] for recent examples). These searches have had to re-invent the way that particles are reconstructed in multipurpose experiments like ATLAS or CMS, to bypass trigger constraints, re-purpose standard reconstruction algorithms and control unusual backgrounds (such as cosmic rays or beam-induced activity). These dedicated searches can be correspondingly complex and time-consuming. Nevertheless, much progress has been made in recent years, and constraints on the production cross-sections (times branching fraction) of LLP production against the lifetime are set. Summary plots that give an overview of the experimental situation, for example for HS models can be found in Ref. [18] for ATLAS and Ref. [19] for CMS.

However, despite this progress, the low-lifetime (or equivalently, early-decay) regime remains ill-covered. Many models have no constraints set by the multipurpose experiments in the region of $c\tau$ (the speed of light times mean proper lifetime) that straddles prompt and displaced decays. This is ostensibly because of the difficulty in reconstructing secondary vertices and the presence of sometimes overwhelming SM backgrounds such as multijet production. In this paper, we argue that existing measurements of prompt processes at the LHC can be used to constrain LLP production: whatever the mean proper lifetime of an exotic LLP, the decay distribution is a falling exponential, and therefore, some fraction of LLPs will behave like prompt particles. Hence, some LLP signatures might already have been visible in well-studied final states for which precision measurements exist at ATLAS and CMS, and can therefore be excluded without the need for a dedicated search. This would liberate person power to study the significantly displaced regions in more detail, making better use of ATLAS and CMS analyst resources. We will describe a method for estimating these constraints using existing open source software, and produce new limits on a variety typical benchmark LLP models which are studied at the LHC, sometimes constraining the same models in the low-lifetime region for the very first time.

The rest of this paper is organised as follows. Section 2 reviews the established CONTUR method to extract constraints on new-physics models from the existing bank of LHC measurements. Section 3 describes how this method normally breaks down for LLP models, and describes a proof-of-principle workflow to remedy this drawback. Sections 4, 5, 6 and 7 then illustrate the application of the modified method to several benchmark LLP models commonly probed by ATLAS and CMS LLP searches, extracting new constraints which complement the direct search programme. The models are chosen to illustrate a breadth of experimental signatures: they include examples of single production and pair production; leptonic and hadronic decays; and scenarios where the LLP is electrically charged or neutral. Our choice of template models and parameter ranges is not guided by theoretical considerations. Instead we choose to work with models which are already employed by LHC experimental collaborations to be able to establish comparisons with existing searches. Finally, we present our conclusions in Section 8.

2 Re-interpretation of measurements with Contur

There exist broadly two ways to extract constraints on new models using existing LHC results. The first is to embed the original benchmark model (on which constraints have been set by an experimental paper) within a wider theoretical framework (examples include SMOBELS [20] or standalone analyses like Ref. [21]). The second option is to determine the kinematics of new final states predicted by a model, and approximate the signal efficiency for this new model in a target analysis. This can be achieved using either efficiency maps provided by the experimental collaborations, or runnable code snippets which reproduce the signal region, if necessary with relevant smearing applied to approximate the effect of the detector. In the latter category, many open source tools provide libraries of re-interpretable analyses, usually exploiting searches. One tool however, makes use instead of the bank of detector-corrected measurements at the LHC, thus avoiding the need to approximate the detector response (often the most costly and approximate step). This method also benefits from the fact that measurement papers almost invariably provide experimentalist-produced definitions for the signal regions in the RIVET [22] library, which is by construction synchronised with the digitized measurement information on the HEP-DATA [23, 24] analysis preservation portal. This tool is called CONTUR [25, 26], and is able to provide rapid insights into constraints on new models (see Refs. [27–29] for recent examples using models predicting new prompt particles).

The CONTUR workflow is detailed in Ref. [26] but the key points are summarised here. The starting point is a new physics model encapsulated in the standard Universal FeynRules Output (UFO) format [30]. The UFO can be passed to a Monte Carlo Event Generator (MCEG) (with suitable model parameter choices) to produce HEPMC [31] files, which contain the particle-level history of the interaction for a given number of generated collision events, after hadronisation. In the next step, the HEPMC events are analysed in RIVET, passing them through dozens of “routines” that encapsulate the definitions of the fiducial regions of as many measurements of SM processes. The result is a set of histograms in the YODA [32] format which show where the signal would have shown up in the LHC measurements. Since RIVET is automatically synchronised with HEPDATA, it is trivial to then compare the size of the new signal (stacked on SM predictions) to the measured cross-sections in each bin, within the experimental uncertainties. The final step is to run a statistical analysis, grouping measurements into orthogonal pools (defined by final state, experiment and centre-of-mass energy) to avoid double counting, and produce a CLs [33] exclusion value. CONTUR acts as a book-keeping and steering layer for this workflow, and provides the final statistical analysis. The power of this method is that while a dedicated search for a new signal with ATLAS or CMS can take years, existing constraints can already be determined in a few days using CONTUR. Indeed, running CONTUR on a single set parameter point takes usually a few hours, and a grid of a few hundred parameter points can easily be done overnight on a standard batch computing farm.

The same method can also be used to extract estimates of the constraints on a given model after the end of the high-luminosity LHC (HL-LHC) lifetime in an automated way, as first demonstrated in Ref. [27]. Indeed, if we assume that 3000/fb are collected by the

end of the HL-LHC programme, we can scale the uncertainties by the square root of the ratio of the increase in integrated luminosity for a given analysis and recalculate the CLs values. Indeed, statistical uncertainties scale with the square root of integrated luminosity. The extrapolation relies on the assumption that experimental systematic uncertainties would also scale this way, which can be deemed a little optimistic. This optimistic assumption is counterbalanced by pessimistic assumptions that no improvements in theoretical uncertainties would take place in the intervening decades, that no new final states would be measured, and that no additional phase space would be explored. Assuming that the pessimistic and optimistic assumptions cancel out, we can take the HL-LHC extrapolations from CONTUR with a certain degree of confidence so long as these caveats are kept in mind.

3 Adapting Contur to LLP topologies

Until now, the CONTUR method has not been usable for LLP signatures. Indeed, the definitions of the analysis signal regions encapsulated in RIVET always assume prompt behaviour (as they should, since the measured SM processes are prompt). Hence, the detector corrections for those analyses would not account for jets or tracks that would be lost due to a displaced starting point. The consequence is an over-estimate of the selection efficiency for LLP signals, and hence unreliable CLs exclusions. For this reason, models (or regions of the model space) predicting LLPs could not be probed using the technique described in Section 2. This prohibition is easier to state than to enforce however: it may not be immediately obvious to a user what combinations of parameters would lead to particles with small widths and therefore long lifetimes. Indeed, the width of a particle can depend on the interplay between the masses of daughter and mother particles, and the values of various couplings and masses of new particles. When performing a scan over a range of parameters in a model with CONTUR, it is not trivial to determine which regions should be avoided, unless special care is taken, as was done for example in Ref. [34]. A workflow to automatically detect LLPs in new models and apply a specific treatment is clearly beneficial to the CONTUR method. Conversely, if such a special treatment can be determined, then it opens the door to probing LLP models with CONTUR.

We propose the following approach to treat LLPs in the RIVET and CONTUR machinery. The basic idea is to evaluate, for a given set of model parameters, what the lab-frame decay length distribution is for all particles with small widths (and therefore long lifetimes) as determined by the event generator. We can then determine what fraction of particles decayed early enough to be treated as prompt. These fractions can be used to calculate a scale factor, with which to down-weight the signal yields predicted by the RIVET routines. The rest of the CONTUR workflow can then run normally. We have implemented a “naive” version of this workflow as a proof of concept, with which we have extracted new constraints on LLP models as discussed in Sections 4, 5, 6 and 7. We discuss at the end of this section how similar results could be achieved more efficiently, but the purpose of this implementation is to show the power of the method and highlight the kind of new constraints that can be obtained. We will now review the step-by-step implementation of our naive method, including technical details.

Step 1 A regular CONTUR scan on a pair of parameters of a model is performed, resulting in a YODA file for each point in the grid. We ensure that the events (in HEPMCs format) are kept rather than deleted, as they normally would be to save disk space.

Step 2 At each point in the grid, the generator log files are parsed to determine the list of particle species, in terms of their unique particle data group identifier (PDGID), which have small widths and therefore macroscopic decay lengths. If one already knows which particles are LLPs in the model, one need only save the width of those particles at this stage. But alternatively, one can select all particles with a width less than $\sim 10^{-6}$ eV (for displacements above the millimeter scale).

Step 3 For the list of LLP PDGIDs at each point, we parse the HEPMC files to extract the LLP kinematics for each event, such that time dilation factors can be calculated. Multiple particle species can be long-lived at a given point, and there can be multiple instances of each species in a given event. For each LLP, a random decay length is calculated, sampling from a falling exponential distribution whose mean is the inverse of that particle species' width (as saved in Step 2). The time dilation factor for that particular particle is applied to obtain a lab-frame decay position for each LLP, separately for each event. In principle, this step can be performed by the MCEG programme, but we choose to do it by hand such that we can treat the lifetime as an independent parameter.

Step 4 We determine a “prompt threshold” p_{th} before which particles can be considered indistinguishable from prompt. Indeed, if the decay of the LLP takes place before p_{th} , then tracks and deposits from the decay products should be reconstructible using the standard ATLAS and CMS algorithms. To choose the value of the threshold, we are guided by Refs. [35] and [36] and the fact that vertices can only be reconstructed in ATLAS and CMS up to about 10 cm in the barrel and around 60 cm in the end-caps. If a vertex cannot be reconstructed, then tracks cannot be either, and the same goes for jets that are typically vetoed in the standard algorithms if they do not contain any tracks. We therefore choose p_{th} to be 10 cm for particles in the barrel ($|\eta| < 1.5$, where η is the pseudo-rapidity) and 60 cm for particles in the endcaps ($|\eta| \geq 1.5$).

Step 5 For each particle species, we build up the distribution of lab-frame decay positions across all generated events. Multiple LLPs of the same species in the same event can contribute to the distribution, assuming that their decay positions are uncorrelated in the lab frame. We then calculate the fraction of LLPs of species i where the decay is below the prompt threshold, to calculate a “prompt fraction” f_i :

$$f_i = \frac{\sum_{j=0}^{N_i} (L^j < p_{th})}{N_i}$$

where N_i is the number of LLPs of species i in the sample (there can be multiple per event), and L^j is the lab-frame decay position of LLP j in either the transverse or longitudinal direction. If the pseudorapidity of the LLP satisfies $\eta_j < 1.5$, then the transverse decay

position is taken and it is compared with the transverse prompt threshold; otherwise if $\eta_j \geq 1.5$, the longitudinal decay position and prompt threshold are used.

Step 6 We then calculate an overall scale factor s taking the product of prompt fractions across species. To account for the fact that LLPs of a same species can occur multiple times per event, the prompt fractions are exponentiated by the average number of LLPs of species i per event. Finally:

$$s = \prod_{\text{species}}^i f_i^{\frac{N_i}{N_{\text{events}}}}.$$

The purpose of s is to scale the final predicted yields to those that would have been obtained if the unreconstructable events were filtered out before processing in RIVET.

Step 7 The resulting s is calculated separately for each model parameter point in the scan, and the corresponding YODA file is scaled by that factor. This has the effect of reducing the predicted signal yields according to the chance that the LLPs in that part of parameter space would have decayed promptly enough to be reconstructed and selected in the standard measurements.

Step 8 The rest of the CONTUR pipeline is executed as normal on the scaled YODA files. The effect of this method is always to decrease the exclusion determined by CONTUR: s is always less than 1 by construction. Effectively, we are down-weighting the claimed CONTUR sensitivity in regions where LLPs can occur. Further, this method is likely somewhat conservative: since we apply the same scale factor uniformly to the output histograms of all measurements, we are assuming that all of the selections would rely specifically on the reconstruction of all the LLPs to select an event. In reality there may be other prompt objects in an event that might cause it to be selected even if the LLPs were not reconstructed. Nevertheless, we prefer to be over-conservative for this proof of principle.

More efficient workflows to achieve similar results can be envisaged. For example, as the HEPMC event format is capable of recording vertex positions calculated by the MCEG, one could bypass Step 3. Further, instead of calculating a scale factor as in Step 6, it would be possible to remove events containing unreconstructible particles completely, for example using the PYHEPMC [37] python module. Another possible option is to build a pipeline that discards individual particles that are displaced (rather than removing the whole event), ensuring that only prompt particles get used in the RIVET routines. This would be a less conservative solution, but requires a much more complex implementation. These alternative approaches can be considered fully in RIVET internally if it allows an earlier processing stage that scans particles' vertices before running the routines. We leave these workflows to be further investigated in future studies.

Finally, since this method takes the same final states that would be predicted by a model, and down-weights the predicted yields, it does not incur any additional model dependence. Further constraints on LLP models could likely be obtained from the other interactions that are possible in the same model, but do not involve LLPs. A good example is if a pair of LLPs is produced from the decay of a scalar mediator, which can be produced

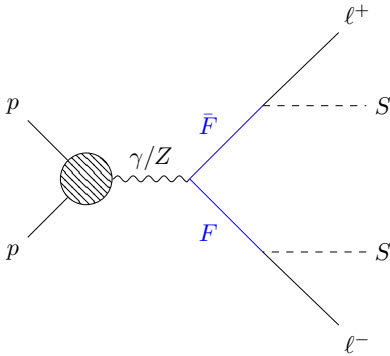


Figure 1: Diagram for the main production process for FIMPs at the LHC, assuming the leptonic version of the model. The blue lines and text indicate the long-lived particle(s).

via gluon–gluon fusion, then that same mediator must necessarily be able to decay back into gluons (and with no LLPs involved at all in that reaction). One could then check the standard dijet measurements and searches for the corresponding bump at the scalar mediator mass. This second method, involving only prompt particles, could then use the standard CONTUR workflow without any special treatment, but it would involve additional assumptions on what is or is not allowed by a particular model. We do not explore this avenue further, and reserve it for future work.

4 Constraints on feebly interacting DM

To illustrate how the method described in Section 3 can be used to obtain new constraints on LLP models, we first consider a simple freeze-in model explaining the observed DM abundance through the decay of an electrically- and/or colour-charged long-lived parent particle into a Feebly Interacting Massive Particle (FIMP), as proposed in Contribution 6 of Ref. [38] and described in more detail in Ref. [39]. Freeze-in is an alternative to the frozen-out Weakly Interacting Massive Particle (WIMP) picture which, despite its attractive features, is under some tension with null experimental evidence. This FIMP model introduces a real scalar DM candidate, denoted S , which is neutral under the SM gauge group. Additionally, a vector-like fermion F plays the role of mediator. In this model, F is electrically charged and can acquire a long lifetime if the coupling governing its decay is small. We consider here the leptonic version of this minimal freeze-in model, where the DM candidate is coupled to the SM through Yukawa-type terms involving the vector-like fermion and the SM charged leptons. The LHC signature of the leptonic model is then the Drell–Yan pair-production of the vector-like fermion (with electric charge ± 1), followed by its decay into the scalar DM candidate along with a charged lepton, as shown in Figure 1. This last decay can be displaced or even take place outside the detector. Another version of the model, where F decays hadronically, exists but is not studied further here.

This FIMP model was confronted with LHC search results in Ref. [38, 39] for different assumptions of LLP lifetime: an ATLAS search for prompt leptons and missing transverse momentum [40] was used for short lifetimes, CMS searches for displaced leptons [41] or

displaced tracks [42] were used for intermediate lifetimes, and an ATLAS search for heavy stable charged particles [43] was used for detector-stable LLPs. Together, these searches provided coverage for $c\tau$ values ranging from tens of micrometers to kilometers, excluding LLP masses between about 150 GeV and 350-700 GeV depending on the lifetime.

To determine any additional constraints that could be extracted from existing measurements using CONTUR, we simulated the process encoded in the publicly available UFO file for the model [44] using MADGRAPH5_AMC@NLO v3.4.2 [45] and PYTHIA v8 [46] for hadronisation. For each point, 10 000 events were generated. The grid was composed of LLP masses in the range of 100 to 1000 GeV in steps of 45 GeV. The lifetime of the F was assumed to be independent of its mass, and 20 values of $c\tau$ were scanned on a logarithmic scale between 0.01 mm and 10 m. The mass of the DM candidate was set to 12 KeV, although the analysis presented here is not strongly sensitive to this choice. Since the LLP F is electrically charged, it would in principle form a reconstructible track before its decay. After the decay, a SM charged lepton may continue the track, but since the unseen s is emitted, one would expect the track from the F/ℓ to be “kinked”: in other words for the hits not to be aligned in the expected pattern for a charged particle trajectory, but instead be the discontinuous union of two curved tracks. Such signatures would be thrown away by ATLAS and CMS, as standard tracking algorithms look for a single particle trajectory. If the decay takes place before the end of the inner tracking system however, the lepton track would still be reconstructed as normal. The values for the prompt threshold described in Section 3 are therefore still applicable. We then follow the procedure set out previously to determine the exclusions from CONTUR.

The results are shown in Figure 2, indicating that F masses from 100 GeV up to ~ 250 GeV can be excluded with 95% confidence level (CL) so long as the mean proper lifetime times the speed of light is below ~ 20 cm. The colours in the figure represent the type of measurement that brings the exclusion power: for masses below about 300 GeV, the exclusion is dominated by analyses that produce two (different-flavour) leptons and missing transverse momentum. For higher masses, other final states dominate the exclusion, notably opposite-flavour leptons with missing transverse energy and the presence of one or more jets, or alternatively measurements of dilepton production with an additional photon. Focusing on the excluded region, taking a point where the mass of F is approximately 150 GeV, Figure 2 also shows the exclusion histogram from the ATLAS measurement of W^+W^- production [49] that generated the highest exclusion. Indeed, the presence of such a signal would have significantly altered the predicted the shape of the spectrum.

In Figure 3, we compare the results obtained from CONTUR to limits derived from direct searches in Ref. [38]. In this case, the direct searches provide more stringent exclusions at high LLP masses, which is perhaps not surprising given that they were originally searches for high-mass supersymmetric particles, and would be more optimal in such a regime. However, all these searches have a cut-off around 150 GeV below which they do not set exclusions. This region is filled in by the CONTUR exclusion lines. Further, the projection of these exclusions to the HL-LHC indicate that even without new searches, the limits on the FIMP model could be extended up to around 600 GeV and to $c\tau$ up to around 4 m, if the same measurements are repeated during the HL-LHC era.

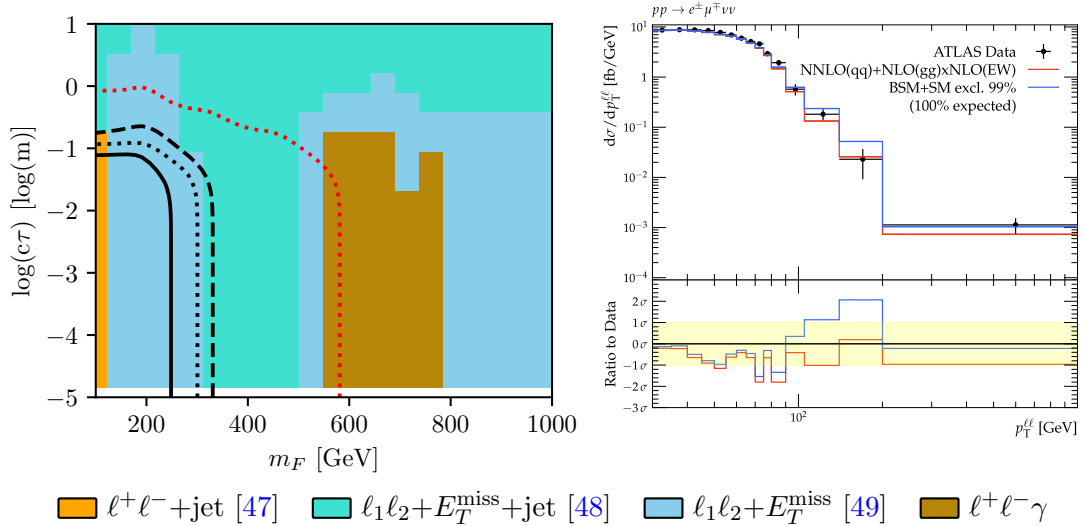


Figure 2: (Left) Exclusion contours for the FIMP model as a function of the F mass and logarithm of $c\tau$, assuming $m_S = 12$ keV. The solid (dotted) lines represent the observed (expected) exclusions at 95% CL. The dashed line represents the observed 68% CL exclusion. The red dotted lines represent the 95% CL expected exclusion extrapolated to the HL-LHC. The area below the curves is excluded. The colours of the cells represent the dominant analysis pool for each point in the grid. (Right) The dominant exclusion histogram for a particular excluded point, where $m_F = 147$ GeV and $c\tau = 0.06$ m. The exclusion comes from the dilepton invariant mass spectrum measured in the $e\mu\nu\nu$ channel of an ATLAS W^+W^- measurement [49], specifically, Figure 7c of that paper. The black markers represent the observed data, and the red line shows the SM prediction. The blue line shows the SM prediction summed with the new physics prediction, which in this case results in a significant disagreement with the observation.

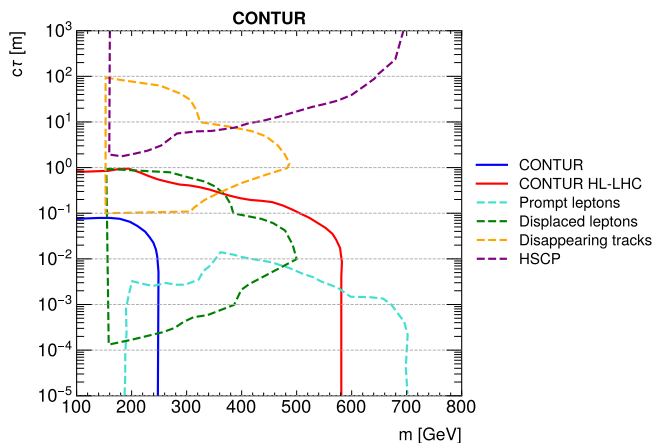


Figure 3: Comparison of CONTUR results with current measurements, extrapolated CONTUR results for HL-LHC, and recasted search results for the FIMP model from Ref. [38].

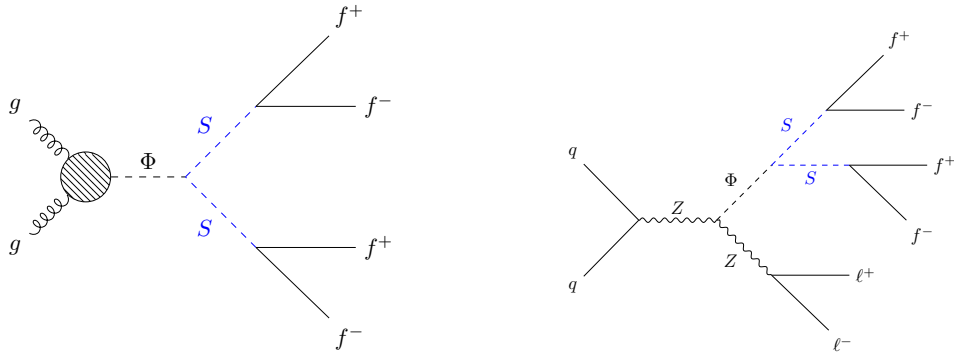


Figure 4: Diagrams for (left) gluon–gluon fusion and (right) associated Z boson production of a HS mediator Φ at the LHC, assuming decays into neutral scalars S , which later decay into fermions f via a Yukawa-type interaction. In this paper, the S decays chiefly into b -quark or t -quark pairs if kinematically allowed.

5 Constraints on hidden sector models with heavy mediators decaying into long-lived scalars

Hidden sector models [7–9, 50] postulate that the SM is connected to a dark sector of new particles via some scalar mediator Φ , which can be the Higgs boson or some new boson. If the mediator is a scalar boson, it can be produced (amongst others) via gluon–gluon fusion (ggF) and associated vector boson production ($V\Phi$) just like the Higgs boson. It can decay into a pair of neutral scalars from the dark sector, denoted S , which would eventually decay back into the SM via a Yukawa interaction, as shown in Figure 4. The S can become long-lived because its decay back into the SM occurs through small couplings. The Hidden Abelian Higgs Model (HAHM) [50, 51] can describe this model. The HAHM introduces two new scalars Φ and S , and a dark photon Z_d . In this section, we focus on the decays of the Φ to S only (as done by ATLAS).

Generic HS models have been studied by both ATLAS and CMS, for example in recent searches for displaced activity in the tracking system [17], calorimeters [14] or muon system [52], ensuring a coverage from millimeters to tens of meters in $c\tau$ of the LLP S , and covering many scenarios for the masses of the particles. Phenomenological reinterpretations of other searches into this model have also been performed, for example in Ref. [53]. Summaries of experimental constraints are available for ATLAS [18] and CMS [19]. CMS has mostly focused on the case where the mediator is the Higgs boson, while ATLAS has also considered heavier mediators, up to 1 TeV in mass. For both experiments, the searches at low lifetimes have studied the $V\Phi$ production mode, exploiting the vector boson for triggering and background reduction. Those searches focused on the Higgs-boson-mediated case. For higher mediator masses, no constraints exist for $c\tau$ below the centimeter range. We address this lack of coverage using the modified CONTUR workflow. We focus on the case of a heavy mediator of mass 1000 GeV produced via associated Z boson production only. The signature consists of pairs of opposite-sign same-flavour leptons in association with up to four b -jets or products of top quark decays if the

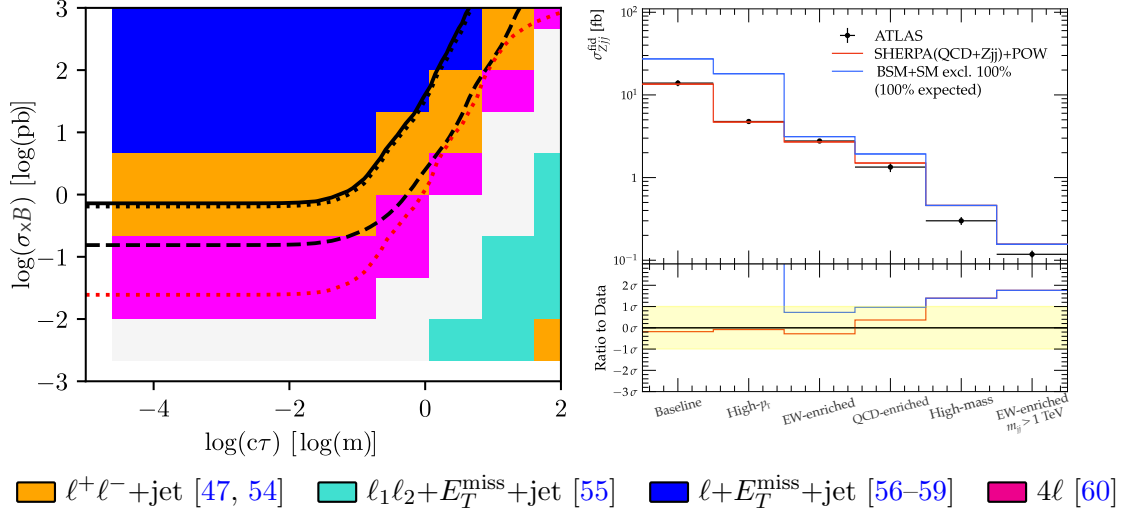


Figure 5: (Left) Exclusion contours for the HS model as a function of the logarithms of cross-section times branching fraction of $Z\Phi(SS)$ and $c\tau$, assuming $m_S = 475$ GeV. The solid (dotted) lines represent the observed (expected) exclusions at 95% CL. The dashed line represents the observed 68% CL exclusion. The red dotted lines represent the 95% CL expected exclusion extrapolated to the HL-LHC. The area above the curves is excluded. The colours of the cells represent the dominant analysis pool for each point in the grid. (Right) The dominant exclusion histogram for a particular excluded point, where the cross-section is around 2.15 pb and $c\tau = 0.31$ m. The exclusion comes from an ATLAS measurement of the cross-section for electroweak production of dijets in association with a Z boson [47], specifically, Table 3 of that paper. The black markers represent the observed data, and the red line shows the SM predictions. The blue line shows the SM prediction summed with the new physics prediction, which in this case results in a significant disagreement with the observation.

LLP mass is above the relevant kinematic threshold. The events are generated with using MADGRAPH5_AMC@NLO v3.4.2 and PYTHIA v8 for hadronisation, using the existing UFO implementation of the HAHM [61] to establish direct comparisons to direct searches. The coupling of the dark photon to the SM and mediator is set to zero. Several values of the neutral scalar S mass are considered, between 50 and 475 GeV, to match the parameter values chosen by ATLAS. The Z boson is allowed to decay into electrons, muons or taus. For each assumption, the grid scan consisted of 10 values of $c\tau$ on a logarithmic scale between 0.01 mm and 100 m, and 10 values of cross-section times branching fraction ($\sigma \times B$) on a logarithmic scale between 0.001 pb and 1000 pb, with 10000 events generated at each point. We note here the high end of the considered cross-sections could be in a non-perturbative regime, but we ignore this effect in this study. The kinematics of the events are assumed to be uncorrelated to the LLP mean proper lifetime, as was done for the ATLAS searches.

The workflow described in Section 3 is exploited to determine what constraints can be extracted from the bank of LHC measurements for HS models with heavy mediators. Since the displaced hadronic activity from LLPs would lead to anomalous jets, which would be

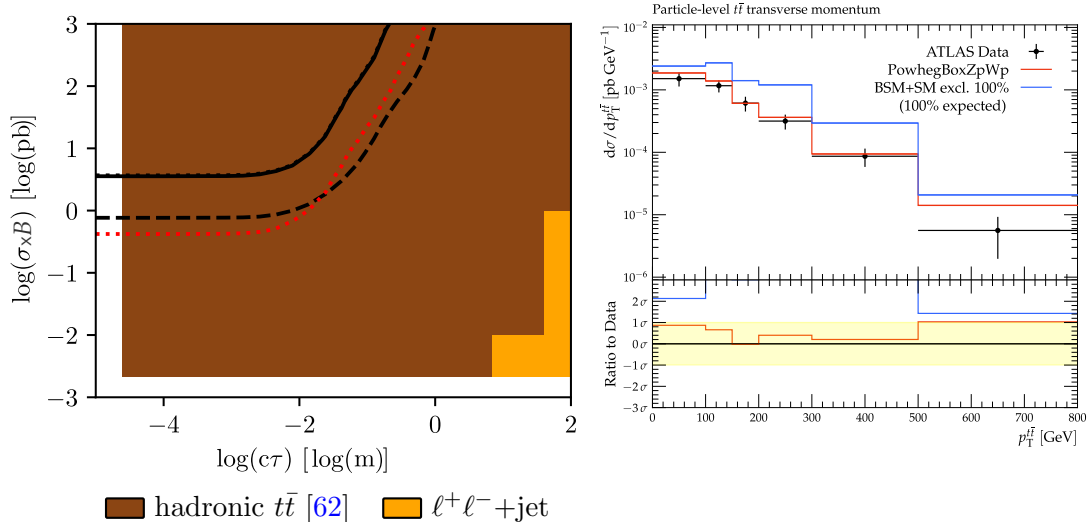


Figure 6: (Left) Exclusion contours for the HS model as a function of the logarithms of cross-section times branching fraction of $Z\Phi(SS)$ and $c\tau$, assuming $m_S = 150$ GeV. The solid (dotted) lines represent the observed (expected) exclusions at 95% CL. The dashed line represents the observed 68% CL exclusion. The red dotted lines represent the 95% CL expected exclusion extrapolated to the HL-LHC. The area above the curves is excluded. The colours of the cells represent the dominant analysis pool for each point in the grid. (Right) The dominant exclusion histogram for a particular excluded point, where the $\sigma \times B$ is around 10 pb and $c\tau = 0.31$ m. The exclusion comes from an ATLAS measurement of boosted $t\bar{t}$ production [47], specifically, Figure 4a of the auxiliary material of Ref. [63]. The black markers represent the observed data, and the red line shows the SM predictions. The blue line shows the SM prediction summed with the new physics prediction, resulting in a significant disagreement with the data.

trackless and therefore vetoed by the standard experimental reconstruction algorithms, we maintain the prompt threshold values described previously. An example of the results for the case where the S mass is set to 475 GeV is shown in Figure 5. In this case, one expects the LLP to decay mostly into top quarks. Cross-sections below around 0.7 pb are excluded up to 10 cm in $c\tau$. The exclusion is mostly driven by 13 TeV ATLAS measurements involving one lepton, missing transverse momentum and jets or measurements of pairs of leptons (from a Z boson decay) and extra jets. Figure 5 focuses on one of the excluded points: the existence of this signal would have caused divergences in the Baseline and High- p_T bins of the measurement presented in Ref [47]. Figure 6 shows equivalent information for a case where the LLP mass is below the top-quark threshold, such that most of the decays are into b -quarks. In this case, the excluded cross-sections peak at around 1 pb for nearly-prompt particles before dropping off after around 2 cm. The dominant analysis is a measurement of $t\bar{t}$ production [62], which would indeed yield the same final state of a pair of leptons accompanied by b -jets.

The comparison of the results using CONTUR with the best results from ATLAS is shown in Figure 7. The regions excluded by CONTUR are exactly those where no constraints

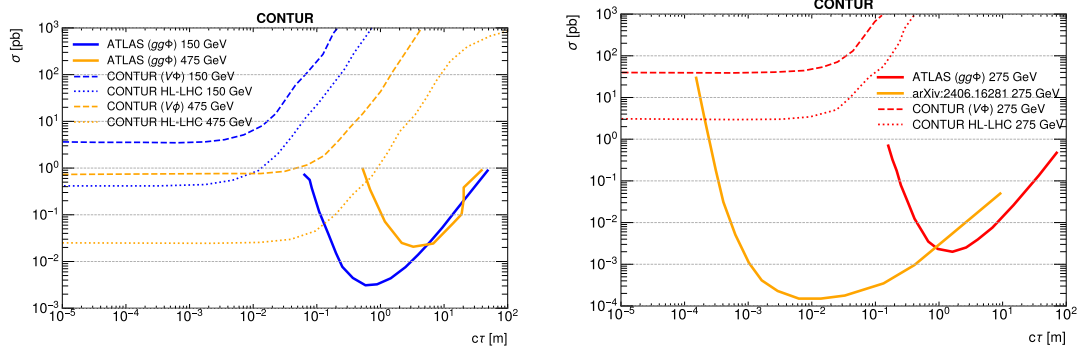


Figure 7: Comparison of CONTUR results for the HS model for a mediator of mass 1 TeV with current measurements, extrapolated CONTUR results for HL-LHC, and comparable results from an ATLAS search [14] and a phenomenological re-interpretation study [53] for the same model and parameter choices.

from direct searches exist. Although for light LLP mass scenarios the CONTUR results are comparatively weak, the results for heavier LLPs are of the same order of magnitude as the direct search and provide complementary constraints in a region which the direct searches were unable to touch.

6 Constraints on heavy, long-lived dark photon models

We now consider a model where the dark photon Z_d is the long-lived particle, as in Refs. [64, 65]. In this model, the Z_d is produced in association with a regular Z boson from the decay of the mediator Φ described in Section 5. It acquires a long lifetime through suppressed couplings to the SM, and decays mostly into quark–antiquark pairs or pairs of leptons. A Feynman diagram showing the processes under study is shown in Figure 8. This model was studied by ATLAS in Refs. [14, 66]. The most constraining results from those searches restrict cross-sections to be smaller than around 0.1 pb in the 10 cm to 10 m range, but no constraints exist so far for $c\tau$ values below 10 cm from ATLAS or CMS.

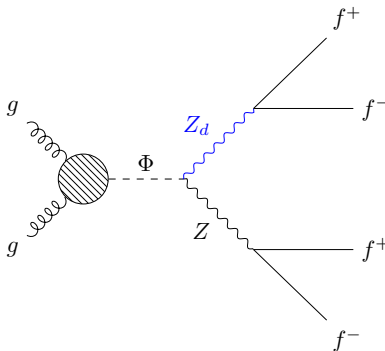


Figure 8: Diagram for the production of a dark photon Z_d via a scalar mediator Φ at the LHC. The blue lines and text indicate the long-lived particle(s).

Events were generated with MADGRAPH5_AMC@NLO v3.4.2 and PYTHIA v8 for hadronisation, starting from the HAHM UFO [61] file used in Section 5 but turning the couplings of the mediator Φ to S particles to zero and setting the S mass to a very high scale. The grid is composed of 10 points spaced logarithmically in $\sigma \times B$ between 0.01 mm and 10 m and 10 points spaced logarithmically in $c\tau$ between 1 mm and 1 km. The cross-section and kinematics of the model are assumed to be independent of the $c\tau$, with 10000 events generated for each combination. Several options of the mediator mass between 400 and 600 GeV, and the dark photon mass between 50 and 400 GeV, are considered, to match those probed by the ATLAS experiment.

The results of the CONTUR study are presented in Figure 9 as a function of $c\tau$ and cross-section times branching fraction, for the case where the mediator mass is 600 GeV and the dark photon mass is 400 GeV. For low lifetimes, the model can be excluded down to the 0.01 pb level, exploiting measurements of the four-lepton invariant mass and dilepton+jets measurements. The sensitivity starts to decrease for $c\tau$ values around 10 cm, in a way that is complementary to the ATLAS search programme. The red dotted line indicates the sensitivity that could be obtained if the measurements were repeated at the high-luminosity LHC, with constraints down to 0.001 pb possible. Figure 9 also shows an example of a histogram from the four-lepton invariant mass measurement [60], where the invariant mass of the second lepton pair further away from the Z boson mass shows a large excess compared with the measured data. So, this model can be excluded by the fact that the dark photon can delay leptonically sufficiently often that it would lead to differences in this spectrum beyond what was measured by ATLAS.

A comparison of the CONTUR results for various mass hypotheses against the results obtained by ATLAS in direct searches can be seen in Figure 10. In this model, the CONTUR results are complementary to the direct searches, effectively ruling out a region not covered by the search programme at a comparable cross-section. Further, measurements at the HL-LHC could even eventually exclude the region covered by the direct searches.

7 Constraints on long-lived photophobic axion-like particles

The final model we consider is a “photo-phobic” axion-like particle (ALP) model where the ALPs couple exclusively to gluons (and so decay into jets), as proposed for example in Ref. [10]. In some parts of the parameter space, the ALP can become long-lived due to small couplings mediating the decay. We consider a case where the ALP is produced via associated Z boson production, as shown in Figure 11. This model was studied by ATLAS in Refs [14, 17] exploiting decays of the ALP in the tracker and calorimeters respectively. The tracker-based search considered ALPs with masses of 40 GeV and 55 GeV, and set constraints at the level of 0.1 pb in the millimeter to 10 cm range. The calorimeter-based search considered ALPs in masses ranging from 100 MeV to 40 GeV, giving constraints for the 40 GeV mass point in the 10 cm to 10 m range. Lighter ALP mass choices give similar constraints but shifted towards lower $c\tau$ values due to increased time dilation factors. In both cases, the sub-millimeter range however is not well covered.

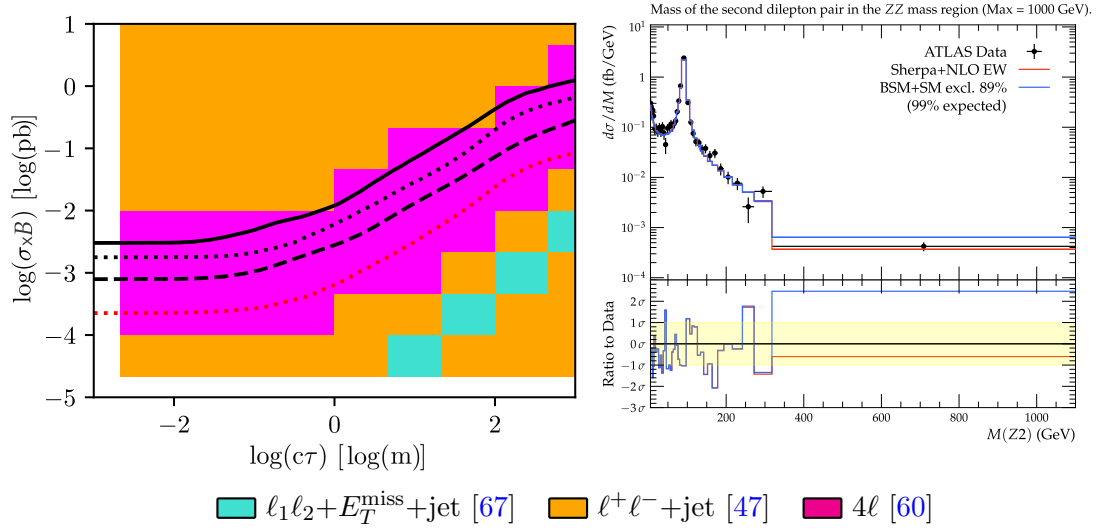


Figure 9: (Left) Exclusion contours for the dark photon model as a function of the F mass and logarithm of the $c\tau$, assuming Φ has a mass of 600 GeV and Z_d has a mass of 400 GeV. The solid (dotted) lines represent the observed (expected) exclusions at 95% CL. The dashed line represents the observed 68% CL exclusion. The red dotted lines represent the 95% CL expected exclusion extrapolated to the HL-LHC. The area above the curves is excluded. The colours of the cells represent the dominant analysis pool for each point in the grid. (Right) The dominant exclusion histogram for a particular excluded point, where $\sigma \times B = 0.001$ pb and $c\tau = 1$ mm. The exclusion comes from a measurement of the four-lepton invariant mass spectrum [60], specifically, from the measurement of the mass of the second lepton pair in Figure 7d of that paper. The black markers represent the observed data, corrected for detector effects, and the red line shows the SM predictions. The blue line shows the SM prediction summed with the new physics prediction, which in this case results in a significant disagreement with the observed data in the last bin.

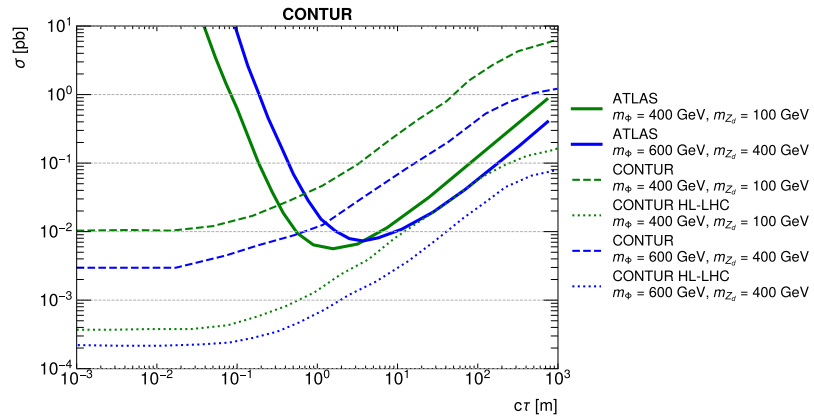


Figure 10: Comparison of CONTUR results for the Z_d model, extrapolated CONTUR results for HL-LHC, and the results of a direct search from ATLAS [14],

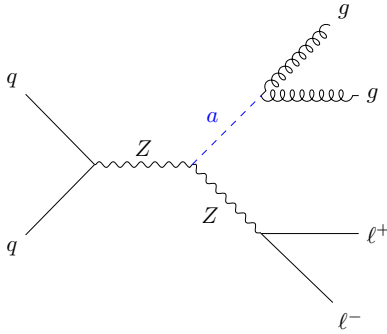


Figure 11: Diagram for the production of an axion-like particle a in association with a Z boson. We consider the case where a decays exclusively into gluons. The blue lines and text indicate the long-lived particle(s).

For the CONTUR study, events were generated using MADGRAPH5_AMC@NLO v3.4.2 and PYTHIA v8 for hadronisation using a UFO file corresponding to the model presented in Ref. [10]. The event generation is limited to cases where the Z decays into electrons or muons, to be consistent with the ATLAS analyses. The grid is composed of 10 points spaced logarithmically in $\sigma \times B$ between 0.1 mm and 10 m and 10 points spaced logarithmically in $c\tau$ between 0.01 mm and 1000 m, with 10000 events generated at each point. The exclusions obtained for this model using CONTUR are shown in Figure 12 for the case where the ALP mass is 10 GeV. The exclusion is dominated by dilepton plus jet analyses everywhere in the plane, as would be expected since the final state under study consists of two light leptons and two gluons. The most sensitive analyses are the Z +jets measurements from ATLAS [47] (the same one already giving exclusion for the HS case in Section 5, but this time in the electroweak-enriched bin) and an equivalent measurement by CMS [68].

A comparison of the CONTUR results with the best-available constraints from ATLAS are shown in Figure 13. They show that the constraints extracted from the measurements are of the same order of magnitude as the direct searches, and completely ruling out the sub-millimeter part of the spectrum in a way that is complementary and competitive with the direct search programme. The plots also show the expected reach of measurements would increase the sensitivity by more than an order of magnitude over the course of the HL-LHC, practically overtaking the existing direct search results.

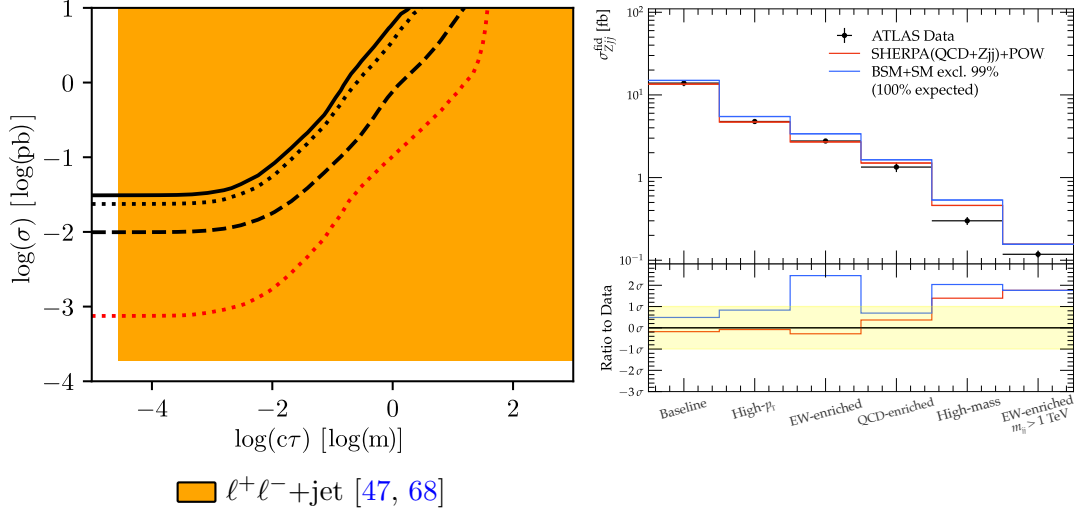


Figure 12: (Left) Exclusion contours as a function of the cross-section times branching fraction for the production of a photo-phobic ALP with a Z boson as a function of the logarithm of the $c\tau$, assuming an ALP mass of 10 GeV. The solid (dotted) lines represent the observed (expected) exclusions at 95% CL. The dashed line represents the observed 68% CL exclusion. The red dotted lines represent the 95% CL expected exclusion extrapolated to the HL-LHC. The area above the curves is excluded. The colours of the cells represent the dominant analysis pool for each point in the grid. (Right) The dominant exclusion histogram for a particular excluded point, where the cross-section is around 0.02 pb and $c\tau = 0.01$ mm. The exclusion comes from an ATLAS measurement of the cross-section for electroweak production of dijets in association with a Z boson [47], specifically, Table 3 of that paper. The black markers represent the observed data, with the red line showing the SM predictions. The blue line shows the SM prediction summed with the new physics prediction, which in this case results in a significant disagreement with the observation.

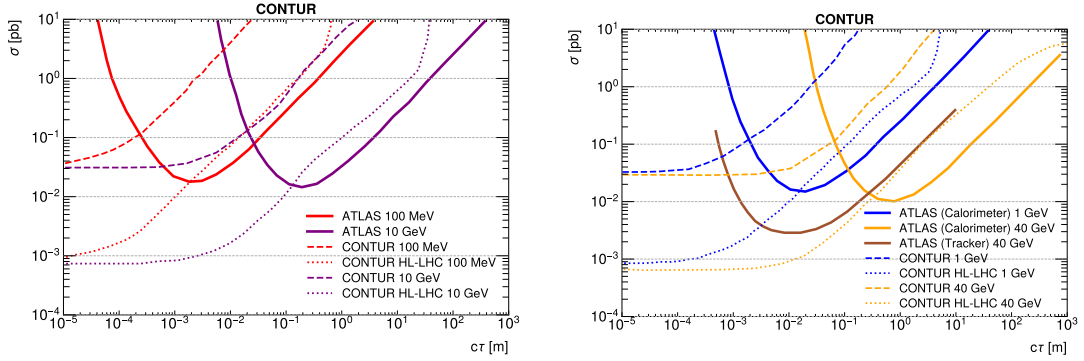


Figure 13: Comparison of CONTUR results for a photo-phobic ALP produced in association with a Z boson, extrapolated CONTUR results for HL-LHC, and dedicated search results from ATLAS exploiting the calorimeter [14] and tracker [17].

8 Conclusions

In this work, a method to constrain long-lived particle models using the fraction of particles that decay early was shown. It exploits the CONTUR method to derive constraints from the bank of LHC measurements, but scaling down the predicted signal yield by the relative fraction of reconstructible long-live particle decays. As a proof of principle, the method was used to determine new constraints on four popular long-lived particle models of various types. The considered models are varied in the nature of the LLPs: charged or neutral, singly-produced or pair-produced, leptonically or hadronically decaying. In each case, new parts of the parameter space can be excluded. Projections of how the constraints could evolve into the HL-LHC era are also presented, which sometimes can match or even overtake direct searches in some parts of the parameter space. This suggests that certain regions need not have dedicated searches, freeing up human resources in the large experimental collaborations to focus on the more displaced regions that cannot be probed in any other way. Moreover, the HL-LHC projections show that large parts of the so far unexplored parameter space could become accessible: in other words, that new long-lived particle discoveries could be awaiting us with the onset of Run 4 of the LHC.

Acknowledgements

We wish to thank Jon Butterworth for fruitful discussions. SJ received funding from the Université Clermont Auvergne Graduate Track for Mathematics and Physics to pursue this research.

References

- [1] N. Arkani-Hamed, A. Gupta, D. E. Kaplan, N. Weiner, and T. Zorawski, *Simply Unnatural Supersymmetry*, [arXiv:1212.6971](#).
- [2] G. F. Giudice and R. Rattazzi, *Theories with gauge-mediated supersymmetry breaking*, *Phys. Rept.* **322** (1999) 419–499, [[hep-ph/9801271](#)].
- [3] R. Barbier et al., *R-Parity-violating supersymmetry*, *Phys. Rept.* **420** (2005) 1–202, [[hep-ph/0406039](#)].
- [4] C. Csáki, E. Kuflik, O. Slone, and T. Volansky, *Models of dynamical R-parity violation*, *JHEP* **06** (2015) 045, [[arXiv:1502.03096](#)].
- [5] J. Fan, M. Reece, and J. T. Ruderman, *Stealth supersymmetry*, *JHEP* **11** (2011) 012, [[arXiv:1105.5135](#)].
- [6] J. Fan, M. Reece, and J. T. Ruderman, *A stealth supersymmetry sampler*, *JHEP* **07** (2012) 196, [[arXiv:1201.4875](#)].
- [7] M. J. Strassler and K. M. Zurek, *Echoes of a hidden valley at hadron colliders*, *Phys. Lett. B* **651** (2007) 374–379, [[hep-ph/0604261](#)].
- [8] M. J. Strassler and K. M. Zurek, *Discovering the Higgs through highly-displaced vertices*, *Phys. Lett. B* **661** (2008) 263–267, [[hep-ph/0605193](#)].

- [9] Y. F. Chan, M. Low, D. E. Morrissey, and A. P. Spray, *LHC Signatures of a Minimal Supersymmetric Hidden Valley*, *JHEP* **05** (2012) 155, [[arXiv:1112.2705](https://arxiv.org/abs/1112.2705)].
- [10] I. Brivio, M. B. Gavela, L. Merlo, K. Mimasu, J. M. No, R. del Rey, and V. Sanz, *ALPs Effective Field Theory and Collider Signatures*, *Eur. Phys. J. C* **77** (2017), no. 8 572, [[arXiv:1701.05379](https://arxiv.org/abs/1701.05379)].
- [11] J. Alimena et al., *Searching for long-lived particles beyond the Standard Model at the Large Hadron Collider*, *J. Phys. G* **47** (2020), no. 9 090501, [[arXiv:1903.04497](https://arxiv.org/abs/1903.04497)].
- [12] **ATLAS** Collaboration, G. Aad et al., *Search for light long-lived neutral particles from Higgs boson decays via vector-boson-fusion production from pp collisions at $\sqrt{s} = 13$ TeV with the ATLAS detector*, [arXiv:2311.18298](https://arxiv.org/abs/2311.18298).
- [13] CMS Collaboration, *Search for long-lived particles using displaced vertices and missing transverse momentum in proton–proton collisions at $\sqrt{s} = 13$ TeV*, *Phys. Rev. D* **109** (2024), no. 11 112005, [[arXiv:2402.15804](https://arxiv.org/abs/2402.15804)].
- [14] **ATLAS** Collaboration, G. Aad et al., *Search for neutral long-lived particles that decay into displaced jets in the ATLAS calorimeter in association with leptons or jets using pp collisions at $\sqrt{s} = 13$ TeV*, [arXiv:2407.09183](https://arxiv.org/abs/2407.09183).
- [15] **CMS** Collaboration, A. Hayrapetyan et al., *Search for long-lived particles using displaced vertices and missing transverse momentum in proton-proton collisions at $s=13$ TeV*, *Phys. Rev. D* **109** (2024), no. 11 112005, [[arXiv:2402.15804](https://arxiv.org/abs/2402.15804)].
- [16] **ATLAS** Collaboration, G. Aad et al., *Search for heavy long-lived multi-charged particles in the full LHC Run 2 pp collision data at $s=13$ TeV using the ATLAS detector*, *Phys. Lett. B* **847** (2023) 138316, [[arXiv:2303.13613](https://arxiv.org/abs/2303.13613)].
- [17] **ATLAS** Collaboration, G. Aad et al., *Search for light long-lived particles in pp collisions at $\sqrt{s} = 13$ TeV using displaced vertices in the ATLAS inner detector*, [arXiv:2403.15332](https://arxiv.org/abs/2403.15332).
- [18] **ATLAS** Collaboration, *Long-lived particle summary plots for Hidden Sector and Dark Photon models*, tech. rep., CERN, Geneva, 2022. All figures including auxiliary figures are available at <https://atlas.web.cern.ch/Atlas/GROUPS/PHYSICS/PUBNOTES/ATL-PHYS-PUB-2022-007>.
- [19] “CMS Higgs decays to LLPs summary.” https://twiki.cern.ch/twiki/bin/view/CMSPublic/SummaryPlotsEX013TeV#Higgs_decays_to_long_lived_parti.
- [20] M. M. Altakach, S. Kraml, A. Lessa, S. Narasimha, T. Pascal, T. Reymermier, and W. Waltenberger, *Global LHC constraints on electroweak-inos with SModelS v2.3*, *SciPost Phys.* **16** (2024), no. 4 101, [[arXiv:2312.16635](https://arxiv.org/abs/2312.16635)].
- [21] U. Haisch and L. Schnell, *Long-lived particle phenomenology in the 2HDM+a model*, *JHEP* **04** (2023) 134, [[arXiv:2302.02735](https://arxiv.org/abs/2302.02735)].
- [22] C. Bierlich, A. Buckley, J. Butterworth, C. Gutschow, L. Lonnblad, T. Procter, P. Richardson, and Y. Yeh, *Robust Independent Validation of Experiment and Theory: Rivet version 4 release note*, [arXiv:2404.15984](https://arxiv.org/abs/2404.15984).
- [23] E. Maguire, L. Heinrich, and G. Watt, *HEPData: a repository for high energy physics data*, *J. Phys. Conf. Ser.* **898** (2017), no. 10 102006, [[arXiv:1704.05473](https://arxiv.org/abs/1704.05473)].
- [24] “The HEPData porta.” <https://www.hepdata.net/>.

- [25] J. M. Butterworth, D. Grellscheid, M. Krämer, B. Sarrazin, and D. Yallup, *Constraining new physics with collider measurements of Standard Model signatures*, *JHEP* **03** (2017) 078, [[arXiv:1606.05296](#)].
- [26] A. Buckley et al., *Testing new physics models with global comparisons to collider measurements: the Contur toolkit*, *SciPost Phys. Core* **4** (2021) 013, [[arXiv:2102.04377](#)].
- [27] J. Butterworth, H. Debnath, P. Fileviez Perez, and Y. Yeh, *Dark Matter from Anomaly Cancellation at the LHC*, [arXiv:2405.03749](#).
- [28] M. M. Altakach, J. M. Butterworth, T. Ježo, M. Klasen, and I. Schienbein, *Exploring Contur beyond its default mode: a case study*, in *56th Rencontres de Moriond on QCD and High Energy Interactions*, 4, 2022. [arXiv:2204.10577](#).
- [29] J. Butterworth, J. Heeck, S. H. Jeon, O. Mattelaer, and R. Ruiz, *Testing the scalar triplet solution to CDF's heavy W problem at the LHC*, *Phys. Rev. D* **107** (2023), no. 7 075020, [[arXiv:2210.13496](#)].
- [30] C. Degrande, C. Duhr, B. Fuks, D. Grellscheid, O. Mattelaer, and T. Reiter, *UFO - The Universal FeynRules Output*, *Comput. Phys. Commun.* **183** (2012) 1201–1214, [[arXiv:1108.2040](#)].
- [31] A. Verbytskyi, A. Buckley, D. Grellscheid, D. Konstantinov, J. William Monk, L. Lönnblad, T. Przedzinski, and W. Pokorski, *HepMC3 Event Record Library for Monte Carlo Event Generators*, *J. Phys. Conf. Ser.* **1525** (2020), no. 1 012017.
- [32] A. Buckley, L. Corpe, M. Filipovich, C. Gutsche, N. Rozinsky, S. Thor, Y. Yeh, and J. Yellen, *Consistent, multidimensional differential histogramming and summary statistics with YODA 2*, [arXiv:2312.15070](#).
- [33] A. L. Read, *Presentation of search results: The CL_s technique*, *J. Phys. G* **28** (2002) 2693–2704.
- [34] S. Amrith, J. M. Butterworth, F. F. Deppisch, W. Liu, A. Varma, and D. Yallup, *LHC Constraints on a $B - L$ Gauge Model using Contur*, *JHEP* **05** (2019) 154, [[arXiv:1811.11452](#)].
- [35] **ATLAS** Collaboration, G. Aad et al., *Performance of the reconstruction of large impact parameter tracks in the inner detector of ATLAS*, *Eur. Phys. J. C* **83** (2023), no. 11 1081, [[arXiv:2304.12867](#)].
- [36] **CMS** Collaboration, S. Chatrchyan et al., *Description and performance of track and primary-vertex reconstruction with the CMS tracker*, *JINST* **9** (2014), no. 10 P10009, [[arXiv:1405.6569](#)].
- [37] A. Buckley, P. Ilten, D. Konstantinov, L. Lönnblad, J. Monk, W. Pokorski, T. Przedzinski, and A. Verbytskyi, *The hepMC3 event record library for monte carlo event generators*, *Computer Physics Communications* **260** (2021) 107310.
- [38] G. Brooijmans et al., *Les Houches 2019 Physics at TeV Colliders: New Physics Working Group Report*, in *11th Les Houches Workshop on Physics at TeV Colliders: PhysTeV Les Houches*, 2, 2020. [arXiv:2002.12220](#).
- [39] G. Bélanger et al., *LHC-friendly minimal freeze-in models*, *JHEP* **02** (2019) 186, [[arXiv:1811.05478](#)].
- [40] **ATLAS** Collaboration, G. Aad et al., *Search for electroweak production of charginos and sleptons decaying into final states with two leptons and missing transverse momentum in*

$\sqrt{s} = 13$ TeV pp collisions using the ATLAS detector, *Eur. Phys. J. C* **80** (2020), no. 2 123, [[arXiv:1908.08215](#)].

- [41] **CMS** Collaboration, *Search for displaced leptons in the e - μ channel*, .
- [42] **CMS** Collaboration, A. M. Sirunyan et al., *Search for disappearing tracks as a signature of new long-lived particles in proton-proton collisions at $\sqrt{s} = 13$ TeV*, *JHEP* **08** (2018) 016, [[arXiv:1804.07321](#)].
- [43] **ATLAS** Collaboration, M. Aaboud et al., *Search for heavy charged long-lived particles in the ATLAS detector in 36.1 fb $^{-1}$ of proton-proton collision data at $\sqrt{s} = 13$ TeV*, *Phys. Rev. D* **99** (2019), no. 9 092007, [[arXiv:1902.01636](#)].
- [44] “FIMP model UFO file.” <https://feynrules.irmp.ucl.ac.be/wiki/FICPLHC>.
- [45] J. Alwall, R. Frederix, S. Frixione, V. Hirschi, F. Maltoni, O. Mattelaer, H. S. Shao, T. Stelzer, P. Torrielli, and M. Zaro, *The automated computation of tree-level and next-to-leading order differential cross sections, and their matching to parton shower simulations*, *JHEP* **07** (2014) 079, [[arXiv:1405.0301](#)].
- [46] T. Sjostrand, S. Mrenna, and P. Z. Skands, *A Brief Introduction to PYTHIA 8.1*, *Comput. Phys. Commun.* **178** (2008) 852–867, [[arXiv:0710.3820](#)].
- [47] **ATLAS** Collaboration, M. Aaboud et al., *Measurement of the cross-section for electroweak production of dijets in association with a Z boson in pp collisions at $\sqrt{s} = 13$ TeV with the ATLAS detector*, *Phys. Lett. B* **775** (2017) 206–228, [[arXiv:1709.10264](#)].
- [48] **ATLAS** Collaboration, G. Aad et al., *Measurements of $W^+W^- + \geq 1$ jet production cross-sections in pp collisions at $\sqrt{s} = 13$ TeV with the ATLAS detector*, *JHEP* **06** (2021) 003, [[arXiv:2103.10319](#)].
- [49] **ATLAS** Collaboration, M. Aaboud et al., *Measurement of fiducial and differential W^+W^- production cross-sections at $\sqrt{s} = 13$ TeV with the ATLAS detector*, *Eur. Phys. J. C* **79** (2019), no. 10 884, [[arXiv:1905.04242](#)].
- [50] D. Curtin et al., *Exotic decays of the 125 GeV Higgs boson*, *Phys. Rev. D* **90** (2014), no. 7 075004, [[arXiv:1312.4992](#)].
- [51] J. D. Wells, *How to Find a Hidden World at the Large Hadron Collider*, [arXiv:0803.1243](#).
- [52] **ATLAS** Collaboration, G. Aad et al., *Search for events with a pair of displaced vertices from long-lived neutral particles decaying into hadronic jets in the ATLAS muon spectrometer in pp collisions at $\sqrt{s}=13$ TeV*, *Phys. Rev. D* **106** (2022), no. 3 032005, [[arXiv:2203.00587](#)].
- [53] Z. S. Wang, *Constraining long-lived particles from Higgs decays at the LHC with displaced vertices and jets*, [arXiv:2406.16281](#).
- [54] **ATLAS** Collaboration, G. Aad et al., *Measurements of the production cross-section for a Z boson in association with b -jets in proton-proton collisions at $\sqrt{s} = 13$ TeV with the ATLAS detector*, *JHEP* **07** (2020) 044, [[arXiv:2003.11960](#)].
- [55] **ATLAS** Collaboration, M. Aaboud et al., *Searches for scalar leptoquarks and differential cross-section measurements in dilepton-dijet events in proton-proton collisions at a centre-of-mass energy of $\sqrt{s} = 13$ TeV with the ATLAS experiment*, *Eur. Phys. J. C* **79** (2019), no. 9 733, [[arXiv:1902.00377](#)].
- [56] **ATLAS** Collaboration, G. Aad et al., *Measurements of top-quark pair differential and double-differential cross-sections in the ℓ +jets channel with pp collisions at $\sqrt{s} = 13$ TeV*

- using the ATLAS detector, *Eur. Phys. J. C* **79** (2019), no. 12 1028, [[arXiv:1908.07305](#)].
[Erratum: *Eur.Phys.J.C* 80, 1092 (2020)].
- [57] **CMS** Collaboration, A. M. Sirunyan et al., *Measurement of differential cross sections for the production of top quark pairs and of additional jets in lepton+jets events from pp collisions at $\sqrt{s} = 13$ TeV*, *Phys. Rev. D* **97** (2018), no. 11 112003, [[arXiv:1803.08856](#)].
- [58] **ATLAS** Collaboration, M. Aaboud et al., *Measurements of top-quark pair differential cross-sections in the lepton+jets channel in pp collisions at $\sqrt{s} = 13$ TeV using the ATLAS detector*, *JHEP* **11** (2017) 191, [[arXiv:1708.00727](#)].
- [59] **CMS** Collaboration, V. Khachatryan et al., *Measurement of differential cross sections for top quark pair production using the lepton+jets final state in proton-proton collisions at 13 TeV*, *Phys. Rev. D* **95** (2017), no. 9 092001, [[arXiv:1610.04191](#)].
- [60] **ATLAS** Collaboration, G. Aad et al., *Measurements of differential cross-sections in four-lepton events in 13 TeV proton-proton collisions with the ATLAS detector*, *JHEP* **07** (2021) 005, [[arXiv:2103.01918](#)].
- [61] “HAHM model UFO file.” <https://feynrules.irmp.ucl.ac.be/wiki/HAHM>.
- [62] **ATLAS** Collaboration, M. Aaboud et al., *Measurements of $t\bar{t}$ differential cross-sections of highly boosted top quarks decaying to all-hadronic final states in pp collisions at $\sqrt{s} = 13$ TeV using the ATLAS detector*, *Phys. Rev. D* **98** (2018), no. 1 012003, [[arXiv:1801.02052](#)].
- [63] “Auxiliary Material for ATLAS-TOPQ-2016-09.” <https://atlas.web.cern.ch/Atlas/GROUPS/PHYSICS/PAPERS/TOPQ-2016-09/>.
- [64] D. Curtin, R. Essig, S. Gori, and J. Shelton, *Illuminating Dark Photons with High-Energy Colliders*, *JHEP* **02** (2015) 157, [[arXiv:1412.0018](#)].
- [65] H. Davoudiasl, H.-S. Lee, and W. J. Marciano, *‘Dark’ Z implications for Parity Violation, Rare Meson Decays, and Higgs Physics*, *Phys. Rev. D* **85** (2012) 115019, [[arXiv:1203.2947](#)].
- [66] **ATLAS** Collaboration, M. Aaboud et al., *Search for the Production of a Long-Lived Neutral Particle Decaying within the ATLAS Hadronic Calorimeter in Association with a Z Boson from pp Collisions at $\sqrt{s} = 13$ TeV*, *Phys. Rev. Lett.* **122** (2019), no. 15 151801, [[arXiv:1811.02542](#)].
- [67] **ATLAS** Collaboration, G. Aad et al., *Measurement of the $t\bar{t}$ production cross-section and lepton differential distributions in $e\mu$ dilepton events from pp collisions at $\sqrt{s} = 13$ TeV with the ATLAS detector*, *Eur. Phys. J. C* **80** (2020), no. 6 528, [[arXiv:1910.08819](#)].
- [68] **CMS** Collaboration, A. M. Sirunyan et al., *Measurements of differential Z boson production cross sections in proton-proton collisions at $\sqrt{s} = 13$ TeV*, *JHEP* **12** (2019) 061, [[arXiv:1909.04133](#)].